One-Shot Integral Invariant Shape Priors for Variational Segmentation*

Siddharth Manay[1,**], Daniel Cremers[2], Anthony Yezzi[3], and Stefano Soatto[4]

[1] Lawrence Livermore National Laboratory
smanay.ece98@gtlaumni.org
[2] Siemens Corporate Research
daniel.cremers@siemens.com
[3] Georgia Institute of Technology
anthony.yezzi@gatech.edu
[4] University of California at Los Angeles
soatto@cs.ucla.edu

Abstract. We match shapes, even under severe deformations, via a smooth reparametrization of their integral invariant signatures. These robust signatures and correspondences are the foundation of a shape energy functional for variational image segmentation. Integral invariant shape templates do not require registration and allow for significant deformations of the contour, such as the articulation of the object's parts. This enables generalization to multiple instances of a shape from a single template, instead of requiring several templates for searching or training. This paper motivates and presents the energy functional, derives the gradient descent direction to optimize the functional, and demonstrates the method, coupled with a data term, on real image data where the object's parts are articulated.

1 Introduction

As computational vision continues the transition from low-level representations of knowledge (edges, features) to high-level representations, shape has become a key component in the detection and recognition of objects. Unfortunately, shape is an elusive concept; shape is the object data left after removing all the "uninteresting" (in this context) dependencies: translation, rotation, scale [1], photometry, articulation, class variation, etc.

Fig. 1 briefly illustrates the difficulties that arise when segmenting an object from an image. The varying illumination, textured/noisy background, and similar intensity values in the fore/background make intensity-based segmentation methods alone useless.

* UCRL-CONF-212393. This work was performed under the auspices of the U. S. Department of Energy by Univesity of California Lawrence Livermore National Laboratory under contract No. W-7405-Eng-48. Supported by NSF IIS-0208197, AFOSR F49620-03-1-0095, ONR N00014-03-1-0850.

** Corresponding author can be reached at: Center for Applied Scientific Computing, Lawrence Livermore National Laboratory, P.O. Box 808, L-551, Livermore, CA 94551-9900. (925) 423-7431.

A. Rangarajan et al. (Eds.): EMMCVPR 2005, LNCS 3757, pp. 414–426, 2005.

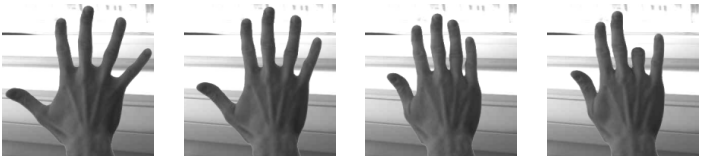

Fig. 1. Similar objects with a variation of its articulated parts. We desire a shape template for segmenting these images that will handle these variations.

A shape template would help; but several templates or a learned probabilistic model of the templates (which in turn requires several templates in the form of a training set) would be needed to segment all the images. Yet humans understand the shape and its variations as well as the backs of their own hands.

This paper proposes to extend the recent work on integral invariant shape descriptors [2, 3, 4] for shapes represented as closed planar contours. These functions are by construction invariant to many of the nuisance factors that make shape analysis difficult (photometry and group actions) and robust to other such nuisances (local deformation of the shape due to articulations or parts, occlusions, or noise). These properties make integral invariants ideal for shape recognition despite nuisances. For the same reasons, integral invariants make ideal candidates for shape templates.

Our contribution is to propose a method for matching shapes undergoing severe deformations, and develop a segmentation scheme that enforces prior shape knowledge through integral invariant representations. This includes using a local representation in terms of an integral invariant signatures, as done by several authors before (reviewed in Sections 1.1 and 2.1), with a smooth re-parametrization of the shape domain to allow for large deformations (Section 2.2). We apply this model to derive an energy functional to enforce shape priors for segmentation (Section 4) and illustrate promising preliminary results for segmentation tasks (Section 5).

1.1 Prior Shapes in Variational Segmentation

Shape has a long history; we only make a few notes on the works that provide context for the interested reader. There are many representations of shape and frameworks for their study, decomposition, and comparison. Statistical methods based landmarks on parameterized contours were pursued in [5, 6, 7, 8]. Representations of shape independent of parameterization began in [9] and continues today [10, 3]. This work ties closely with representations of shape as points on an infinite dimensional manifold, where the deformations are the actions of Lie groups [11, 12, 13, 14, 10]. These approaches based on an explicit representation of shape enable the definition of correspondences between shapes [15, 16, 10].

For variational contour-evolution methods for segmentation [17, 18, 19, 20, 21], a statistical representation of shape is used to cope with class variability [22, 23, 24, 25, 26, 7] Unlike statistical methods which require a training set, we propose a deterministic method that spans these variations with a *single template shape* by exploiting the locality property of an integral invariant. In contrast to some of the literature on shape

where a method is termed group-invariant when the group parameters are an optimized input for the function (i. e. [7]), we call a function invariant if the value is *independent of an action belonging to the group*. (We make this precise in Sec. 2.1.)

2 Integral Invariants and Shape Distance

In this section, we briefly review integral invariants and describe a intuitively meaningful shape distance defined between these invariants.

2.1 Integral Invariants

For a shape represented as a closed planar curve $\gamma : \mathbb{S} \mapsto \mathbb{R}^2$ and a group G acting on $\mathbb{R}^2$, an *integral G-invariant* is an integral function of the curve that does not vary due to the action of any $g \in G$. Formally, for a kernel $h : \mathbb{R}^2 \times \mathbb{R}^2 \mapsto \mathbb{R}$,

$$I_\gamma(p) = \int_{\bar{\gamma}} h(p, x) d\mu(x) \tag{1}$$

is an integral invariant if

$$I_\gamma(p) = I_{g\gamma}(gp) \quad \forall g \in G. \tag{2}$$

These invariants share several desirable qualities of their more well-known cousins, differential invariants, including locality. However, unlike differential invariants, integral invariants are far more robust to noise. Specific examples include the "observed transport" shape measure [2] and the local area invariant [3]. Both of these invariants are parameterized by r, the radius of a circular kernel.

Due to its noise-robustness, we favor the so-called local area Euclidean-invariant. Specifically, the invariant is based on a kernel $h(p, x) = \chi(B_r(p) \cap \bar{\gamma})(x)$, which represents the indicator function of the intersection of a small circle of radius r centered at the point p with the interior of the curve γ. For a radius r, the corresponding integral invariant

$$I^r_\gamma(p) \doteq \int_{B_r(p) \cap \bar{\gamma}} dx \tag{3}$$

can be thought of as a function from the interval $[0, 1]$ to the positive reals, bounded above by the area of the region bounded by the curve γ. Alternately, normalizing the

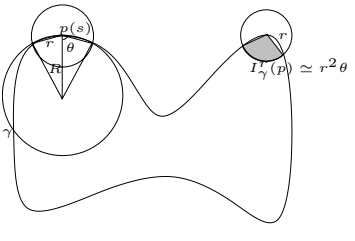

Fig. 2. Integral area invariant defined by eq. (3)

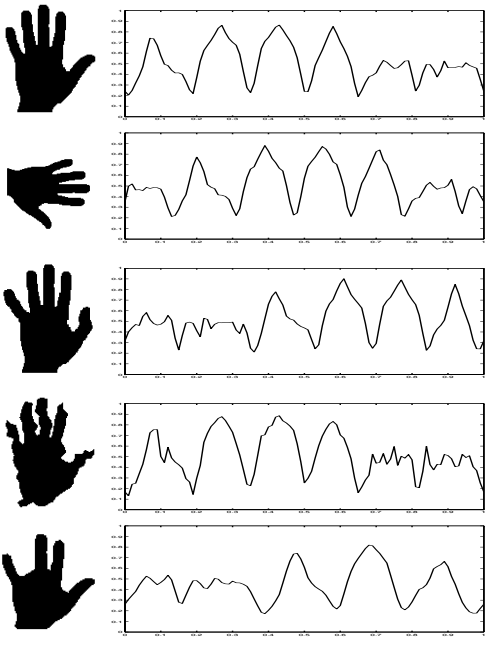

Fig. 3. *Sample shapes and their integral invariants.* Kernel size is 15% of the curve's bounding box. Note the missing "hump" on the last invariant due to the missing arclength (finger) in last row.

functional by the area of B_r maps the interval $[0, 1]$ to $[0, 1]$. This is illustrated in Fig. 2 and examples are shown in Fig. 3, which demonstrates (in the first four rows) the effectiveness of this representation for comparing shapes under Euclidean transformations, articulation of parts, and in global additive noise. However, Fig. 3 (last row) demonstrates that the local area invariant, like all other integral and differential invariants, is not robust to a highly localized perturbation such as an occlusion. In the next section we present a method to warp the parameterization of the curves so that such comparisons can be made robustly.

2.2 Shape Distance and Warping Integral Invariants

While invariants can be designed to be invariant to group actions, and integral invariants are robust to noise, an invariant for highly localized, high energy perturbations of a shape, such as the addition of spikes, slivers, or other parts, or the "disappearance" of parts due to occlusion or change in configuration (i.e. Fig. 3, first, third, and fifth row) is much more problematic. A naive distance defined on an invariant would yield a relatively large distance between the two hands in the last two rows of Fig. 3 (implying they are very different) while intuitively these shapes should have a small distance between them.

From the perspective of invariants, the large difference between shapes with local variation is due to the parameterization of the curves, as demonstrated in Fig. 3. If the "stub" could be mapped to the ring finger (which has much longer arclength), the distance between the two shapes would be limited to the error caused by that finger. This warping of the parameterization of one shape, or more symmetrically both shapes, would allow the computation of an intuitively more satisfying distance while effectively inducing point correspondences between the two curves.

Thus we wish to find an optimal correspondence between the contours and concurrently measure the shape distance based on the correspondence. Intuitively, two corresponding points on two contours should have similar invariant value, which leads us to define the optimal correspondence in terms of an energy functional $E(I_1, I_2, d; s)$ for the discrepancy between two integral invariants I_1, I_2 , in terms of the disparity function $d(s)$, as follows:

$$\begin{aligned} E(I_1, I_2, d; s) &= E_1(I_1, I_2, d; s) + E_2(d'; s) \\ &= \int_0^1 \|I_1(s - d(s)) - I_2(s + d(s))\|^2 ds \\ &+ \alpha \int_0^1 \|d'(s)\|^2 ds \end{aligned} \tag{4}$$

where $\alpha > 0$ is a constant. The first term E_1 of the energy functional measures the similarity of two curves by integrating the local difference of the integral invariant at corresponding points. A cost functional based on a local comparisons minimizes the impact of articulations and local changes of a contour because the difference in invariants is proportionally localized in the domain of the integral; contrast this with a global descriptor where local changes influence the descriptor everywhere. The second term E_2 of the energy functional is associated with the elastic energy of the disparity function $d(s)$ with the control parameter α that penalizes stretching or shrinking of the disparity.

The shape matching of two curves is obtained by finding a correspondence between their integral invariants. The correspondence between two curves is determined by the disparity function $d(s)$ that minimizes the energy functional as follows:

$$d^*(s) = \arg\min_{d(s)} E(I_1, I_2, d; s) \tag{5}$$

Given the correspondence d^*, the shape matching between two curves (γ_1, γ_2) is given as:

$$\gamma_1(s - d^*(s)) \sim \gamma_2(s + d^*(s)), \quad \forall s \in [0, 1] \subset \mathbb{R} \tag{6}$$

where $\sim$ denotes the point-wise correspondence between curves [4].

Suggested methods for the implementation of this optimization include graph-based methods as in [27, 2, 28, 29], where d^* is the shortest path through a graph where the nodes represent pointwise correspondences.

3 Estimating Shape and Correspondence Via Bayesian Inference

In this work, we address the following problem: Given an image $I : \mathbb{R}^2 \to \mathbb{R}$ and given a *single* template shape $\gamma_0 : \mathbb{S} \to \mathbb{R}^2$, determine the optimal segmentation $\gamma : \mathbb{S} \to \mathbb{R}^2$

of the image plane and the optimal correspondence (or reparameterization) function $q : \mathbb{S} \to \mathbb{S}$ which associates the parts of the contour γ with corresponding parts on the template γ_0. (In Section 4 we discuss the connections between the reparameterization $q(s)$ and disparity $d(s)$ in Equation 4.)

Clearly, the estimation of the optimal contour γ and the optimal correspondence function q are highly coupled problems. Therefore we propose to solve this problem by maximizing the conditional probability

$$\mathcal{P}(\gamma, q|I, \gamma_0) \tag{7}$$

simultaneously with respect to both the contour γ and the correspondence function q.

According to the Bayesian formula, we can rewrite (7) as:

$$\mathcal{P}(\gamma, q|I, \gamma_0) = \frac{\mathcal{P}(I|\gamma)\mathcal{P}(\gamma, q|\gamma_0)}{\mathcal{P}(I)}. \tag{8}$$

Here we have made the two assumptions that the conditional probability $\mathcal{P}(I|\gamma, q, \gamma_0)$ in the numerator of (8) does not depend on the given template γ_0 or on the correspondence function q.

Maximizing this conditional probability for a given image I is equivalent to minimize the energy

$$E(I, \gamma, q) = \alpha E_{data}(I, \gamma) + (1 - \alpha)E_{shape}(\gamma, \gamma_0, q), \tag{9}$$

where the data energy and the shape energy correspond to the negative logarithms of the two probabilities given in the numerator of (8). Since the focus of this paper is on modeling a novel shape prior, for simplicity we choose the Chan-Vese energy as a data term, and alternate the minimization of each energy term. In the following, we will focus on modeling the shape energy.

Minimizing the above joint energy will accomplish two goals. The first is to favor segmentation contours γ that separate the domain of the image data I into object and background. The second is to favor contours that have a shape similar to a template contour γ_0. In contrast to existing methods to introduce shape priors into variational segmentation, the proposed shape prior is not learnt as a statistical model inferred from a set of training shapes. We only use a single template shape, and the flexibility of the shape prior arises through the use of a more sophisticated shape dissimilarity measure which can handle stretching or shrinking and the correspondence of subparts.

Based on the assumption that the intensities of object and background are Gaussian-distributed, one can derive a data term E_{data} given by the piecewise constant Mumford-Shah functional [30, 31]:

$$E_{cv}(I, \gamma) = \int_{\bar{\gamma}} (I - c_1)^2 dx + \int_{\Omega/\bar{\gamma}} (I - c_2)^2 dx + \nu \int_{\gamma} ds \tag{10}$$

here c_1, c_2 are the constant approximation of u (i. e. the mean) inside and outside γ. This functional can be minimized by evolving an initial contour and model in the gradient direction

$$\gamma_{t,cv} = ((c_1 - c_2)(I - c_1 + I - c_2) - \nu\kappa)\, \boldsymbol{N} \tag{11}$$

where κ denotes the local curvature. This functional will provide the connection between the segmenting contour γ and the image data. However, any other variational segmentation model proposed in the literature could be substituted.

4 Integral Invariant Templates for Curve Evolution

In this section, we will construct an appropriate shape prior E_{shape} in (9) for variational segmentation based on the notion of integral invariant shape descriptions and pointwise correspondence. Intuitively, we reason that the best way to update the portion of a contour that will become, say, a finger, is to compare it to the relevant part of the template, the corresponding finger. As discussed in Section 2.2, integral invariant based shape distances allow us to do exactly this; with the invariant and correspondence in hand, the evolution of the contour is governed by only the shape of the template, and is not influenced by nuisance factors.

Section 2.2 hints at our design of the energy term that will achieve the second goal. Following [32], which evolves a contour so that its invariant has a certain property, we evolve the contour to reduce its shape distance with a template invariant. This shape term has all the advantages of integral invariant methods: (1) the resulting flow will also be G-invariant, eliminating contour motions that do not instruct the shape of the contour, or alternately eliminating the need to align or register the contour to the template; (2) the resulting flow will be more noise robust; and (3) the resulting flow will be less sensitive to articulation of parts, allowing a template to better represent a class of shapes. For instance, with a method that is not insensitive to articulation, a hand template could only be used when the target hand's fingers *are configured exactly like the template*; with the integral invariant representation of the hand, hands with splayed or bent fingers have similar invariants to the template.

These advantages are realized with a shape energy term

$$E_{shape}(\gamma, \gamma_0, q) = \frac{1}{2}\int_{\gamma} (I(s) - I_0(q(s)))^2 ds \tag{12}$$

based on the integral invariant from Section 2.1 rewritten as

$$I(s) = \int_{\bar{\gamma}} B(\gamma(s) - \tilde{s}, r) d\tilde{s}. \tag{13}$$

$q(s) = s - 2d(s)$ is an asymmetric expression of the warping function. For convenience, we define $f(s) = I(s) - I_0(q(s))$. In anticipation of the time-dependence of the arclength parametrization, we rewrite the energy with a change of variables

$$E(\gamma, q) = \frac{1}{2}\int_{\gamma} f(p)^2 ||\gamma_p|| dp. \tag{14}$$

Taking the time derivative yields

$$E_t(\gamma, q) = \int_{\gamma} f(p) f_t(p) ||\gamma_p|| dp + \frac{1}{2}\int_{\gamma} f(p)^2 ||\gamma_p||_t dp, \tag{15}$$

$f_t(p) = I_t(p) - (I_o(q(p))_t$ The second term is the well known curve shortening flow, so we concentrate on the first term. Two notes at this point aid the simplification of the expression. First, we must compute the derivative of the integral invariant I_t. Via the divergence theorem, an area-based energy of the form $E(s) = \int_{\tilde{\gamma}} F(s)ds$ (for a general function $F(s)$) has a derivative that can be expressed as a contour integral $E_t(s) = \int_\gamma \langle \gamma_t, F(s)N \rangle ds$, where $\langle \cdot, \cdot \rangle$ is the dot product and N is the normal direction. Applying this formula to I_t yields

$$I_t(p) = -\int_\gamma \langle \gamma_t, B(|\gamma(p) - \tilde{s}|, r)N \rangle d\tilde{s} \tag{16}$$

Second, we note that $I_o(\cdot)$ is the constant shape template, so its derivative is 0. Rewriting and reversing the change of variables

$$E_t(\gamma, q) = -\int_\gamma f(s) \int_\gamma \langle \gamma_t, B(|\gamma(s) - \tilde{s}|, r)N \rangle d\tilde{s} ds + \dots \tag{17}$$

Re-arranging the nested integral allows us to introduce another convenient quantity,

$$g(s) = \int_\gamma f(s)B(|\gamma(s) - s|, r)ds, \tag{18}$$

and write

$$E_t(\gamma, q) = \int_\gamma \langle \gamma_t, -\int_\gamma g(s)dsN \rangle d\tilde{s} + \dots \tag{19}$$

Including the omitted curvature shortening term,

$$E_t(\gamma, q) = \int_\gamma \langle \gamma_t, (-\int_\gamma g(s)ds + f(s)^2\kappa)N \rangle d\tilde{s}. \tag{20}$$

In order to maximally reduce this energy, we chose γ_t to be the negative of the second term of the inner product

$$\gamma_t = \int_\gamma (-g(s) + f(s)^2\kappa(s))N. \tag{21}$$

The $g(s)$ term has a straightforward interpretation; at a point on the contour, it is simply the integral of difference of the invariant values on the sections of γ inside the kernel.

In the next section, we integrate this shape term into a segmentation functional.

5 Energy Minimization with Integral Invariant Shape Templates

In this section we will detail how to minimize the joint energy (9) to simultaneously compute a segmentation and a correspondence of the parts of the segmentation to respective parts of the given shape template. We will apply this segmentation functional to real data to demonstrate the flexibility of integral invariant shape templates.

We will minimize the functional (9) with the partial differential equation

$$\gamma_t = \gamma_{t,data} + \alpha\gamma_{t,shape} \tag{22}$$

where $\gamma_{t,shape}$ is (21) and $\gamma_{t,data}$ is the flow in (11). α is a user-defined weighting term.

The curve γ is embedded in a higher-dimensional function $\Phi : \mathbb{R}^2 \mapsto \mathbb{R}$ to make use of the well-known level-set implementation of curve evolution methods [33, 19, 21]. The level-set function is constructed so that $\{x|\Phi(x) = 0\} = \gamma$; the evolution of γ in the $\gamma_t = \beta N$ direction is realized through the evolution of Φ in the

$$\Phi_t = -\beta|\nabla\Phi| \tag{23}$$

direction.

We employ a dual representation of the contour to speed the computations. A polygonal representation is used for the computation of $d(s)$, $f(s)$, and $g(s)$. These terms, computed on the vertices of a polygon, are then mapped to the level-set domain and nearest-neighbor extrapolated. N, κ, the data terms, and Φ_t are computed directly in the image/level-set domain, per usual. At each timestep, we recompute the integral invariant and correspondence, so that we are alternating the two optimizations (correspondence, segmentation).

In the remainder of this section we show an experiment that demonstrates the power of an integral invariant based template over more traditional shape-template methods. Specifically, we will address the case where an affine transformation is not adequate to map the shape template to the object in the image. In this case, a more general, local deformation is required; the goal is to demonstrate that the locality of the integral invariant translates into energy penalties that are proportional to the size of the deformation.

We compare our implementation to a implementation that seeks to optimize the distance from the contour to a shape prior

$$E_{shape}(\gamma) = \int_\gamma d(\gamma(s), g\gamma_0)ds \tag{24}$$

where $g \in G$, a group. For a traditional method that aligns the shape template to the object during the segmentation process, an affine transformation in two dimensions requires the optimization of six parameters. Many methods in the literature restrict themselves to lower-dimensional groups (Euclidean, similarity) but the generalization is straightforward. The optimization is usually implemented with two steps per iteration; first an update of the contour

$$\gamma_{t,shape} = \nabla d(\gamma, g\gamma_0) \tag{25}$$

and second an update of the transformation parameters g. In the remainder of this section, we demonstrate results on real images that show the potential of the integral invariant as a shape template.

Fig. 4 shows the segmentation of the image of a hand, taken with varying illumination against a busy background. While the contrast is strong, it should be noted that the gray values of the object and background are in a similar range, making segmentation by image data alone (via the Chan-Vese method with a strong curvature prior) difficult,

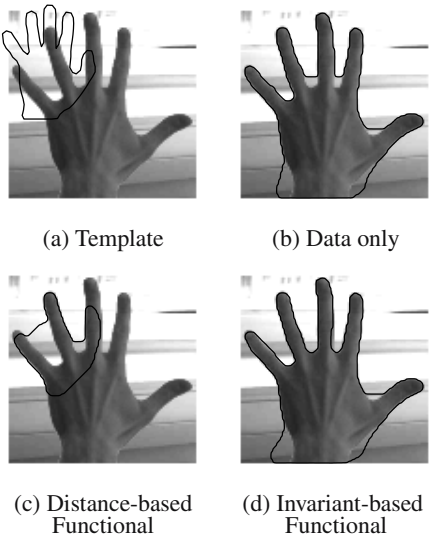

(a) Template (b) Data only

(c) Distance-based Functional (d) Invariant-based Functional

Fig. 4. Segmentation with a shape template. α=0.85.

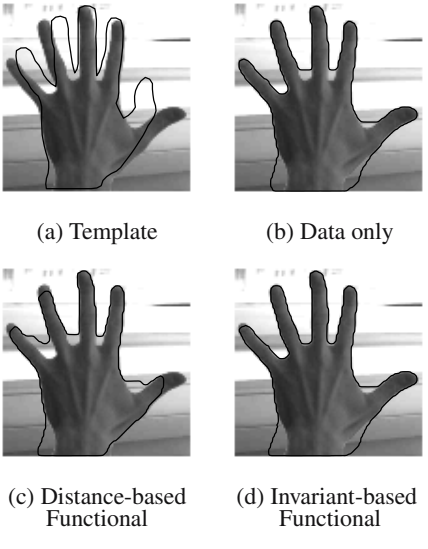

(a) Template (b) Data only

(c) Distance-based Functional (d) Invariant-based Functional

Fig. 5. Segmentation with a shape template. α=0.85.

as shown in Fig. 4(b). A shape template may assist in the segmentation, but the choice of template is important. An unregistered template (as in Fig. 4) has a strong influence on the contour. This is because the segmentation contour cannot both be near the template and edges in the image; the energy functional converges to a "compromise" between the two criteria. Unfortunately, this compromise serves neither criteria well. In contrast,

the integral invariant shape template is not dependent on the location of the template. Regardless of the alignment, the template does not compete with the data term for the location of the contour (d).

Figure 5 shows the added flexibility of the integral invariant shape template. While optimization of transform parameters allows the alignment of the distance function template to the data (a), the template cannot capture the articulated thumb (c). Again, the integral invariant template generalizes to better capture this object (d). Here, due to the locality of the invariant, the deviations of the segmentation from the template are penalized *only at the differing bends in the contour* This allows for a much better "compromise" between the shape and data terms; now a single template shape can be used despite the many variations (finger poses) inherent in this class of object.

6 Open Issues

The method we have proposed relies on the uniqueness of the integral invariant representation. In [3] Manay et. al. outline the relationship between curvature, which is a unique representation of the contour, with the integral invariant in the limit as kernel size goes to 0. For finite kernel size the uniqueness of the invariant is the topic of continuing investigation.

If the invariant is not unique, the contour flow will not necessarily converge to the shape template, but may converge to other shapes that have the same invariant. Indeed, this may explain the instabilities we have observed in the contour flow in synthetic experiments where the image data term is discarded. However, in practice, the data terms of the flow help restrict the contour to the desired solution. A more rigorous solution would be to base the flow on an integral invariant that is unique; the development of which is also the topic of our continuing research.

7 Summary and Conclusions

In this paper we draw on the emerging work on local integral invariant shape descriptions to first present a shape distance between two contours based on optimal correspondences between the parts of the contours that have similar integral invariant. Based on this shape distance we construct a shape energy functional for variational segmentation. This new shape energy term fundamentally differs from previously proposed statistical shape priors which allow for shape deformations that are statistically learnt from an entire set of training shapes. Our shape prior only uses a single template shape, it is not dependent on the relative position and rotation of the template, eliminating the need for registration of the data to the template. Further, due to the locality properties of the integral invariant, the more sophisticated shape distance allows for certain deformations of the given template, such as local stretching or shrinking and the articulation of parts. Preliminary results show the effectiveness of integral invariant templates in a curve evolution segmentation framework implemented via level set methods and applied to real data.

References

1. Kendall, D.G.: The diffusion of shape. Advances in Appl. Probability **9** (1977) 428–430
2. Pitiot, A., Delingette, H., Toga, A., Thompson, P.: Learning Object Correspondences with the Observed Transport Shape Measure. In: Information Processing in Medical Imaging IPMI'03. (2003)
3. Manay, S., Hong, B., Yezzi, A., Soatto, S.: Integral invariant signatures. In: European Conf. Comp. Vis. (2004)
4. Manay, S., Hong, B., Cremers, D., Yezzi, A., Soatto, S.: Integral invariants and shape matching. Pat. Anal. and Mach. Intell. (2005) Submitted.
5. Bookstein, F.: The Measurement of Biological Shape and Shape Change. Springer, New York (1978) volume 24 of *Lect. Notes in Biomath.*
6. Cootes, T.F., Taylor, C.J., Cooper, D.M., Graham, J.: Active shape models – their training and applications. Comp. Vision Image Underst. **61** (1995) 38–59
7. Cremers, D., Osher, S., Soatto, S.: Kernel density estimation and instrinsic alignment for knowledge-driven segmentation: Teaching level sets to walk. In: DAGM. (2004)
8. Dryden, I.L., Mardia, K.V.: Statistical Shape Analysis. Wiley, Chichester (1998)
9. Fréchet, M.: Les courbes aléatoires. Bull. Inst. Int'l Stat. **38** (1961) 499–504
10. Klassen, E., Srivastava, A., Mio, W., Joshi, S.H.: Analysis of planar shapes using geodesic paths on shape spaces. Pat. Anal. and Mach. Intell. **26** (2004) 373–383
11. Grenander, U.: Lectures in Pattern Theory. Springer, Berlin (1976)
12. Grenander, U., Chow, Y., Keenan, D.M.: Hands: A Pattern theoretic Study of Biological Shapes. Springer, New York (1991)
13. Trouvé, A.: Diffeomorphisms, groups, and pattern matching in image analysis. Int. J. Computer Vision **28** (1998) 213–221
14. Younes, L.: Computable elastic distances between shapes. SIAM J. Appl. Math **58** (1998) 565–586
15. Basri, R., Costa, L., Geiger, D., Jacobs, D.: Determining the similarity of deformable shapes. Vision Research **38** (1998) 2365–2385
16. Gdalyahu, Y., Weinshall, D.: Flexible syntactic matching of curves and its application to automatic hierarchical classication of silhouettes. Pat. Anal. and Mach. Intell. **21** (1999) 1312–1328
17. Kass, M., Witkin, A., Terzopoulis, D.: Snakes: Active contour models. Int. J. Computer Vision **1** (1987) 321–323
18. Kichenassamy, S., Kumar, A., Olver, P.J., Tannenbaum, A., Yezzi, A.: Analysis of planar shape influnce in geodesic active contours. In: Int. Conf. Comp. Vis. (1995) 810–815
19. Chan, T., Vese, L.: Active contours without edges. IEEE Trans. on Image Proc. **10** (2001) 266–277
20. Caselles, V., Kimmel, R., Sapiro, G.: Geodesic active contours. In: Int. Conf. Comp. Vis. (1995) 694–699
21. Tsai, A., Yezzi, A., Willsky, A.: Curve evolution implementation of the Mumford Shah functional for image segmentation, denoising, interpolation, and magnification. IEEE Trans. on Image Proc. **10** (2001) 1169–1186
22. Leventon, M.E., Grimson, W.E.L., Faugeras, O.: Statistical shape influence in geodesic active contours. In: Proc. Conf. Comput. Vision and Pat. Rec. Volume 1. (2000) 316–323
23. Tsai, A., Yezzi, A., Wells, W., Tempany, C., Tucker, D., Fan, A., Grimson, E., Willsky, A.: Model-based curve evolution technique for image segmentation. In: Proc. Conf. Comput. Vision and Pat. Rec. (2001) 463–468
24. Chen, Y., Tagare, H., Thiruvenkadam, S., Huang, F., Wilson, D., Gopinath, K.S., Briggs, R.W., Geiser, E.: Using shape priors in geometric active contours in a variational framework. Int. J. Computer Vision **50** (2002) 315–328

25. Rousson, M., Paragios, N.: Shape priors of level set represenations. In: European Conf. Comp. Vis. (2002) 78–92
26. Rousson, M., Paragios, N., Deriche, R.: Implicit active shape models for 3D segmentation in MRI imaging. In: Int. Conf. Medical Image Computing and Computer Assited Intervention. (2004) 209–216
27. Bakircioglu, M., Grenander, U., Khaneja, N., Miller, M.I.: Curve matching on brain surfaces using frenet distances. Human Brain Mapping **6** (1998) 329–333
28. Sebastian, T., Klein, P., Kimia, B.: Alignment-based recognition of shape outlines. Lecture Notes in Computer Science **2059** (2001) 606–??
29. Tomasi, C., Manduchi, R.: Stereo without search. In: European Conf. Comp. Vis. (1996) 452–465
30. Mumford, D., Shah, J.: Optimal approximations by piecewise smooth functions and associated variational problems. Comm. on Pure and Applied Math. **42** (1989)
31. Zhu, S.C., Yuille, A.: Region competition: Unifying snakes, region growing, and Bayes/MDL for multiband image segmentation. Pat. Anal. and Mach. Intell. **18** (1996) 884–900
32. Nain, D., Yezzi, A., Turk, G.: Vessel segmentation using a shape driven flow. In: Int. Conf. Medical Image Computing and Computer Assited Intervention. (2004)
33. Osher, S., Sethian, J.: Fronts propagating with curvature dependent speed: Algorithms based on Hamilton-Jacobi formulations. J. of Comp. Physics **79** (1988) 12–49